ISSN 8756-6990, Optoelectronics, Instrumentation and Data Processing, 2020, Vol. 56, No. 1, pp. 10–18. © Allerton Press, Inc., 2020.
Russian Text © The Author(s), 2020, published in Avtometriya, 2020, Vol. 56, No. 1, pp. 13–22.

ANALYSIS AND SYNTHESIS OF SIGNALS AND IMAGES

Specific Features of Spectral Properties of Volume Reflection Holograms of Diffuse Objects

E. F. Pen*

Institute of Automation and Electrometry, Siberian Branch, Russian Academy of Sciences, pr. Akademika Koptyuga 1, Novosibirsk, 630090 Russia
**E-mail: pen@iae.nsk.su*

Received September 16, 2019; revision received October 7, 2019; accepted for publication October 8, 2019

Abstract—Specific features of spectral properties of volume reflection holograms are determined, namely, broadening of the spectral response (reflex) contour toward both the short-wave and long-wave spectral ranges in the case where the angle of incidence of the white-light probing beam differs from the direction of reference wave propagation in hologram recording. This effect is essentially different from the known angular dependence of the reflex of the elementary volume reflection grating. A theoretical explanation for experimental data is provided, and formulas are derived, which are used to calculate the transmission spectra of the studied gratings. These spectra are found to be qualitatively consistent with the experiment.

Keywords: optical holography, volume reflection gratings, Bragg diffraction, photopolymers.

DOI: 10.3103/S8756699020010021

INTRODUCTION

The properties of elementary volume reflection holograms (gratings) were described in detail in the classical papers [1, 2], where, in particular, the spectral and angular dependences of the diffraction efficiency of these holograms on the recording material thickness, modulation amplitude of the refractive index, correlation of the Bragg conditions of recording/reconstructing, and other factors were studied.

The simplest way to obtain a volume reflection grating is to use the known scheme [3, 4], where the laser radiation (reference beam) passes through the recording medium and illuminates the object, which can be, e.g., a usual mirror reflecting the radiation in the reverse direction and, thus, forming the object beam interfering with the reference beam.

In this case, the grating period determining the wavelength of the spectral response resonance (reflex) in the case of probing with white light depends on the wavelength of the recording laser radiation and on the angle of incidence of the reference beam. The grating reflex contour usually has the form of a narrow spectral band whose center is shifted only to the short-wave range as the probing beam incidence angle is varied.

If the mirror in this scheme is replaced by a white diffuse object (e.g., gypsum surface or mat-surface photographic paper), then the reflected (scattered) radiation can be presented as a set of plane waves with a certain angular distribution. Interfering with the reference wave, each of these waves generates its own reflection grating. It should be noted that this example is similar in many aspects to the so-called "noise gratings" arising due to interference of the laser radiation incident onto the recording material with numerous waves formed after scattering of this radiation on material inhomogeneities [6, 7]. As applied to transmission holograms, noise gratings were studied in much detail both theoretically and experimentally. In particular, it was demonstrated that they lead to the emergence of a pattern of diffraction rings [6] and reduce the hologram efficiency [8].

At the same time, the spectral properties of volume reflection holograms of diffuse objects were not studied in detail in the past, especially in the case of mismatch of the Bragg conditions of recording/reconstruction [1].

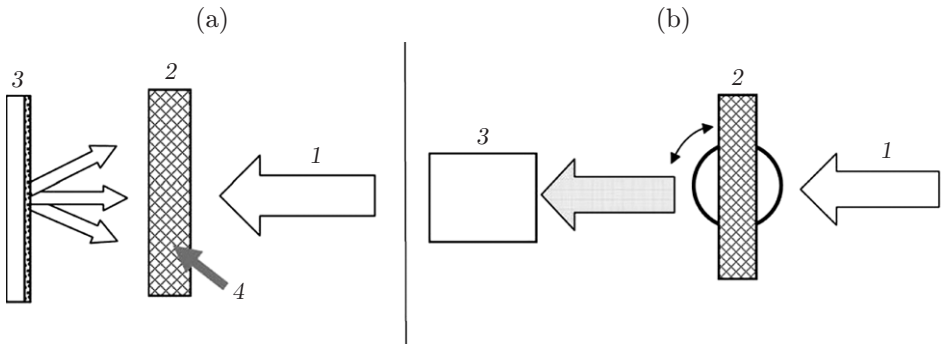

Fig. 1. Test setups: (a) recording a volume reflection hologram of diffuse objects; (b) measurements of their spectral responses.

Such a study seems to be fairly important because this mismatch can lead to distortions of the color balance of reconstructed images in artistic and protective holograms, and also holographic displays [9].

The goal of the present activity was to perform an experimental and theoretical study of the spectral properties of volume reflection holograms of diffuse objects with different parameters of their recording and reconstruction.

EXPERIMENTAL INVESTIGATIONS

The test setups used in the present study are schematically shown in Fig. 1. The elements in Fig. 1a are the collimated laser beam (*1*), recording medium (*2*), recorded object (*3*), and simplified spatial structure of the volume reflection hologram (*4*). The elements in Fig. 1b are the probing white light beam (*1*), examined hologram (grating) mounted on a rotating table for changing the probing beam incidence angle (*2*), and digital spectrophotometer (*3*) (in the present experiments, we used an AvaSpec-ULS2048 spectrophotometer produced by Avantes, the Netherlands). This is a standard procedure for testing volume reflection gratings [10, 11].

First we fabricated reflection grating No. 1, and the object was a flat metallic mirror. The reference beam of the DPSS laser (with the wavelength $\lambda_0 = 532$ nm and intensity of 2 mW/cm^2) was directed normal to the surface of the recording material, which was taken to be a holographic photopolymer (BAYFOL HX TP from the series of products of Bayer MaterialScience AG (Germany) [11] with the recording layer thickness $L = 55$ μm, which made it possible to fabricate phase holographic gratings with a high diffraction efficiency. The mirror was located behind the photopolymer tightly pressed to the latter. The recording energy was 60 mJ/cm^2. Then we fabricated a reflection hologram No. 2; in this case, the object was white mat-surface photographic paper (LOMOND Matt). The recording energy was also 60 mJ/cm^2.

For all holograms, matching of the Bragg conditions of recording/reconstruction had to be provided to prevent distortions of reconstructed images (in particular, the incidence angles of the reference and reconstructing beams had to be identical). Unfortunately, this requirement is seldom fully satisfied in practice, especially in the case of illumination of volume reflection holograms by white light. Therefore, it is necessary to study the dependences of possible distortions in the case of mismatch of the hologram recording/reconstruction conditions. For this purpose, we obtained the transmission spectra of the fabricated holograms for different angles ψ of incidence of the reconstructing (probing) white light radiation with respect to the reference beam direction in hologram recording. Figure 2a shows the spectra of grating No. 1 for $\psi = 0$, 5, and 10° (curves *1*, *2*, and *3*, respectively). Such measurements are commonly known and were performed by many researchers (e.g., [5, 10]).

It is seen that the spectral response contour for grating No. 1 in the case of the probing beam incidence angle $\psi = 0°$ is narrow (the contour width is ~4 nm at a level of 0.5 of the transmission minimum); the central wavelength of the resonance is $\lambda_r = 529$ nm and is shifted only to the short-wave range with a change in the angle ψ in accordance with the law $\lambda_r = \lambda_0 \cos\psi$ [5]. It is important to note that the spectrum contour width remains almost unchanged. The 3-nm difference of the resonance wavelength from the expected value $\lambda_0 = 532$ nm is explained by the well-known influence of effective shrinkage of the photopolymer [12], which

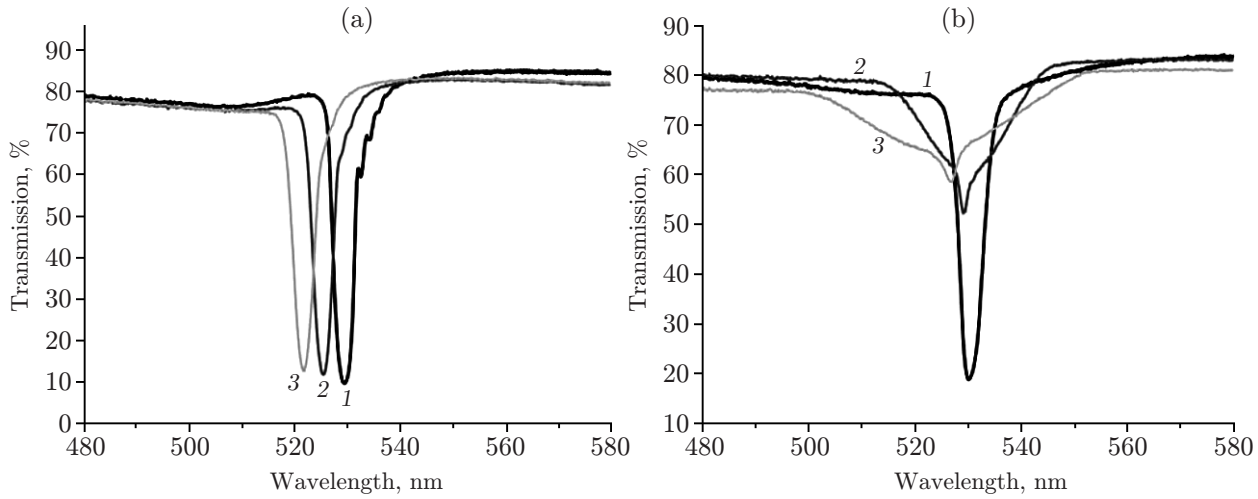

Fig. 2. Transmission spectra of gratings for difference incidence angles of the probing radiation: (a) grating No. 1; (b) grating No. 2.

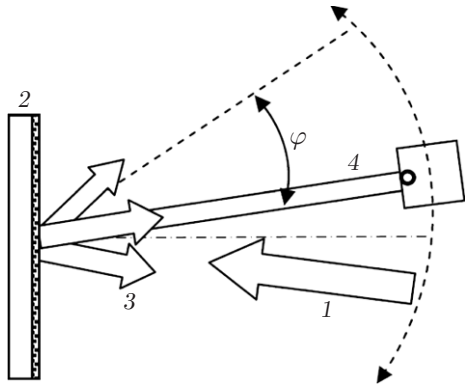

Fig. 3. Setup for measuring the angular distribution of scattered light.

is approximately −0.5% for the material used in the study and is responsible for decreasing of the reflex wavelength.

The transmission spectra of hologram No. 2 is essentially different (Fig. 2b). Even for the probing beam incidence angle $\psi = 0^\circ$ (curve *1*), the contour width is slightly greater than that of grating No. 1 and significantly increases with an increase in the angle ψ: $\psi = 5^\circ$ (curve *2*) and $\psi = 10^\circ$ (curve *3*); moreover, the broadening contour extends to both the short-wave and long-wave ranges with respect to the center of the spectral response (reflex), which is accompanied by reduction of the contour depth. For example, for $\psi = 10^\circ$, the contour width near its base is ∼50 nm. As far as the author is aware, such features were not observed earlier and have to be analyzed.

Obviously, the spectral properties and diffraction activity of the examined reflection holograms of diffuse objects depend on the angular distribution of scattered light. Such a distribution was obtained on a test setup schematically shown in Fig. 3. It consists of a collimated laser beam with a finite (cut) Gaussian distribution of the transverse profile of intensity, which was incident onto the object at an angle of ∼10° with respect to the normal to the object surface (*1*), diffuse object (white mat-surface photographic paper) (*2*), scattered light beams (*3*), and photodetector with the input diaphragm 1 mm in diameter mounted on a rotating platform (*4*). The object was located at a distance $L = 100$ mm from the photodetector; the ratio of the incident beam intensity and the maximum intensity of reflected light was ∼ 600 : 1 and ∼ 10 : 1 near the paper plane.

Figure 4 shows the normalized intensity of reflected (scattered) light as a function of the angle φ between the directions of the current observation and the maximum signal of reflected light (the points are the experimental data). This plot coincides fairly well with the approximating curve of the Gaussian function

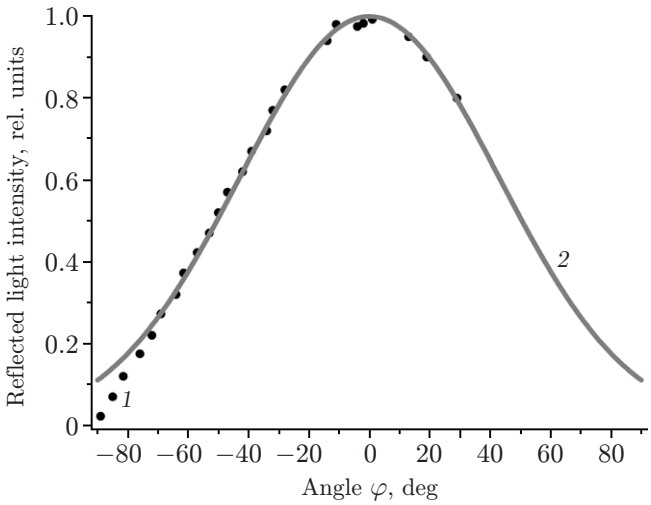

Fig. 4. Normalized intensity of reflected (scattered) light versus the angle φ.

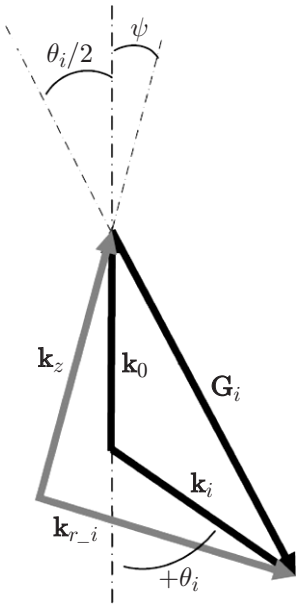

Fig. 5. Geometric pattern of the vectors of the reference $\mathbf{k}_0$, object $\mathbf{k}_i$, probing $\mathbf{k}_z$, and reconstructed $\mathbf{k}_{r\_i}$ beams with respect to the subgrating vector $\mathbf{G}_i$.

(curve *2*), and the measurement error is within ±2%. It should be noted that this dependence describes the intensity of the object beams interfering with the reference beam in recording hologram No. 1.

THEORETICAL POSTULATES AND NUMERICAL DATA

Let us consider the geometric scheme of the beam vectors obtained in recording and reconstructing the reflection holograms of diffuse objects (Fig. 5), where $\mathbf{k}_0$ is the reference beam vector, $\mathbf{k}_i$ is the vector of the ith beam of reflected radiation, which is further called the object beam, $|\mathbf{k}_0| = |\mathbf{k}_i| = 2\pi n/\lambda_0$, λ_0 is the wavelength of laser radiation used for grating recording in air, $\mathbf{G}_i = \mathbf{k}_i - \mathbf{k}_0$ is the vector of an individual grating (subgrating) formed due to interference of the object i and reference beams in the recording material with a refractive index n, $|\mathbf{G}_i| = 2\pi/\Lambda_i$ is the absolute value of this vector, where Λ_i is the spatial period of the grating, $\mathbf{k}_z$ is the probing beam vector, and $\mathbf{k}_{r\_i}$ is the vector of the reconstructed wave corresponding to the Bragg condition $\mathbf{G}_i = \mathbf{k}_i - \mathbf{k}_0 = \mathbf{k}_{r\_i} - \mathbf{k}_z$.

Let α_i be the angle between the vectors $\mathbf{k}_0$ and $\mathbf{k}_i$, and let the reference beam be incident normal onto the object surface. Then the scattered (reflected) ith beam forms an angle $\theta_i = 180^\circ - \alpha_i$ to this normal. In this case, we have

$$\Lambda_i = \lambda_0/(2n\cos(\theta_i/2)).$$

The number of object beams is extremely large; however, it is possible to identify beams with different values of the scattering angles in the radial direction θ_i, $i = 1, 2, \ldots, N_\theta$, and also in the azimuthal direction ω_j, $j = 1, 2, \ldots, N_\omega$. Clearly, subgratings with different values of ω_j, but identical values of θ_i have the same period Λ_i.

If the probing beam of white light is directed to the ith subgrating along its vector, then it can be easily found that the reconstructed radiation wavelength is

$$\lambda_{r\_i} = \lambda_0/\cos(\theta_i/2), \tag{1}$$

i.e., it is greater than the laser radiation wavelength λ_0. When the probing beam is aligned at an angle ψ with respect to the reference beam direction in recording the grating, as is illustrated in Fig. 5, then one can apply the results of [5] to demonstrate that the wavelength of the reflex of the ith subgrating changes and becomes equal to

$$\lambda_{r\_i} = \lambda_0\cos(\theta_i/2 + \psi)/\cos(\theta_i/2). \tag{2}$$

It is seen from Eq. (2) that the wavelength of the grating reflex wavelength can only decrease with variation of the probing beam incidence angle ψ in the case with $\theta_i = 0^\circ$ (i.e., when the reference and object beams in Fig. 1 propagate rigorously toward each other). However, at $\theta_i \neq 0^\circ$, the wavelength of the reflex of the ith subgrating can both decrease and increase as compared to the central value calculated by Eq. (2) (formula (2) is analyzed below).

To estimate the degree of reflection of the entire set (i, j) of reflection subgratings, we first consider the spatial structure of the ith grating, which can be presented, following [5, 13], as a set of pairs of thin dielectric layers a and b with thicknesses h_a and h_b repeated with the period Λ_i. The number of pairs of the layers is $P_i = L/\Lambda_i$. The refractive indices of these layers n_a and n_b should correspond to the distribution of the energy of illumination of the pattern of interference of the reference and ith beams. Assuming that the hologram recording process as a result of this illumination is linear, a photoinduced harmonic distribution of the refractive index is created in the photopolymer:

$$n_i(x) = n_0 + \Delta n_i\cos(2\pi x/\Lambda_i).$$

Here Λ_i is the period of the interference pattern; n_0 and Δn_i are the mean value and the amplitude of modulation of the refractive index of the photopolymer, which also depend on the contrast (visibility) V of the interference pattern. It is known [1, 2] that $V = 2\sqrt{S}/(1+S)$, where S is the ratio of the interfering beam intensities. Let us replace the real half-tone interference pattern by a binary distribution of light intensity. Then the contrast of grating No. 1 is $V = 1$, whereas the maximum and minimum values of the refractive index correspond to $n_0 + \Delta n = n_a$ and $n_0 - \Delta n = n_b$, where n_0 and Δn are reference data: $n_0 = 1.5$ and $\Delta n \sim 0.02{-}0.04$ [10, 11].

For a set of gratings applied in the same volume of the recording material, the value of Δn have to be divided in proportion to their number and the visibility V of the interference pattern of each grating should be taken into account. Therefore, the refractive indices of the layers a and b of an individual subgrating for hologram No. 2 can be expressed as

$$n_a = n_0 + \frac{\Delta n}{N_\theta N_\omega}\frac{2\sqrt{S_{i,j}}}{1+S_{i,j}}; \quad n_b = n_0 - \frac{\Delta n}{N_\theta N_\omega}\frac{2\sqrt{S_{i,j}}}{1+S_{i,j}}. \tag{3}$$

The reflection coefficient $R_{i,j}(\lambda)$ or transmission coefficient $T_{i,j}(\lambda) = 1 - R_{i,j}(\lambda)$ of the i, jth subgrating can be found as a function of the probing beam wavelength by the following formulas [5, 13]:

$$R_{i,j}(\lambda) = |r_{i,j}(\lambda)|^2, \qquad r_{i,j}(\lambda) = \frac{(m_{11} + m_{12}n_0)n_0 - (m_{21} + m_{22}n_0)}{(m_{11} + m_{12}n_0)n_0 + (m_{21} + m_{22}n_0)} \tag{4}$$

($m_{11,\ldots,}m_{22}$ are the elements of the total transfer matrix M of the i, jth grating).

In turn, $M = (M_{ab})^P$, where M_{ab} is the transfer matrix for the pair of layers a and b of this grating, which is equal to the product of the transfer matrices of each layer [13]:

$$M_{ab} = \begin{bmatrix} \cos\varphi_a & -in_a^{-1}\sin\varphi_a \\ -in_a\sin\varphi_a & \cos\varphi_a \end{bmatrix} \begin{bmatrix} \cos\varphi_b & -in_b^{-1}\sin\varphi_b \\ -in_b\sin\varphi_b & \cos\varphi_b \end{bmatrix}.$$

Here $\varphi_{a,b} = 2\pi n_{a,b}h_{a,b}/\lambda$ is the phase incursion of the light wave with the wavelength λ from one boundary of the layers a and b to the other.

The total reflection coefficient of the entire set of subgratings can be written as

$$R(\lambda) = \sum_{i,j}^{N_\theta,N_\omega} R_{i,j}(\lambda). \tag{5}$$

As axially aligned subgratings with an identical index i are identical, one can replace expressions (3) by

$$n_a = n_0 + \frac{\Delta n}{N_\theta}\frac{2\sqrt{S_i}}{1+S_i}, \qquad n_b = n_0 - \frac{\Delta n}{N_\theta}\frac{2\sqrt{S_i}}{1+S_i}$$

and skip summation with respect to j in formula (5); then

$$R(\lambda) = \sum_{i=-N_\theta}^{N_\theta} R_i(\lambda). \tag{6}$$

Figure 6 shows the calculated transmission spectra of grating No. 2 as a set of subgratings for different values of the probing beam incidence angle. The presentation of the calculated results in the form of transmission rather than reflection spectra is caused only by the convenience of comparisons with the above-mentioned experimental data. For the same reason, the calculated transmission values of the gratings were multiplied by a correction factor equal to 0.8 because the resultant holograms possess significant residual absorption of light by photopolymer components (see Fig. 2). It should be also noted that the reflection coefficient of the hologram is actually the measure of its diffraction efficiency.

In the calculations, we consider the number of beams $N_\theta = +25, \ldots, -25$ that fall into the interval of the angles $\theta_i = +40^\circ, \ldots, -40^\circ$ containing more than 60% of the scattered light energy. Hereinafter, all values of the angles are given for the air environment. The calculated range of variation of S extends from $\sim 10:1$ (for $\theta_i = 0^\circ$) to $\sim 100:1$ (for $\theta_i = \pm 40^\circ$). At $\psi = 0^\circ$, when the probing beam incidence angle coincides with the reference beam incidence angle in hologram recording, i.e., the Bragg conditions are satisfied for all

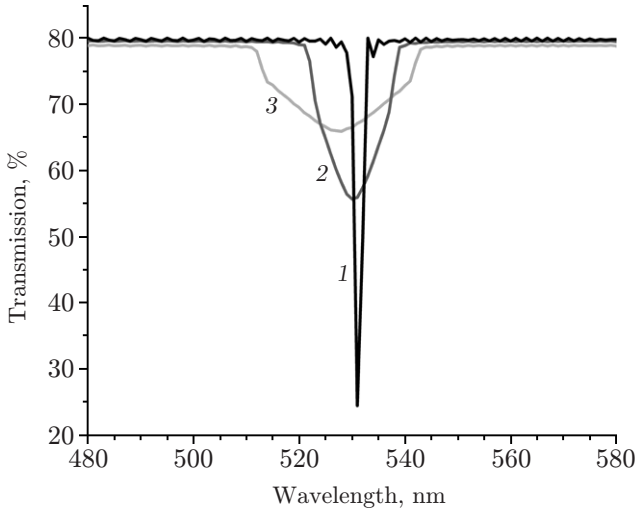

Fig. 6. Transmission spectra of grating No. 2 for different values of the probing beam incidence angle: $\psi = 0$ (*1*), 5 (*2*), and 10° (*3*).

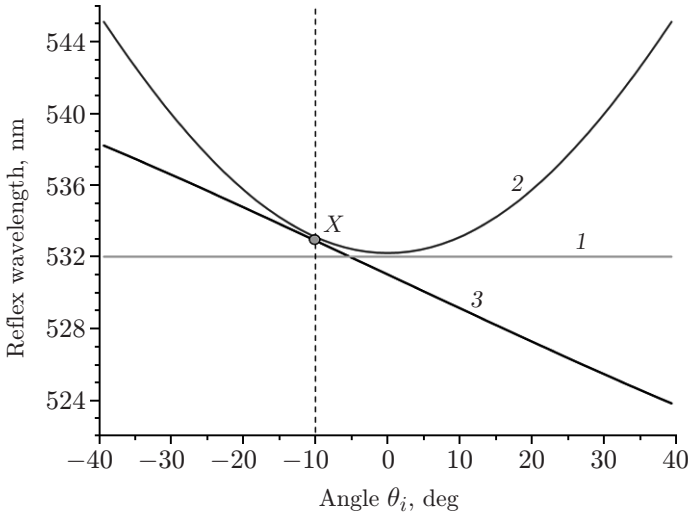

Fig. 7. Variations of the subgrating reflex wavelength for different values of θ_i.

subgratings, the total reflex is formed with the spectrum in the form of a deep and narrow contour whose central value is close to the wavelength of the recording radiation (the influence of shrinkage was ignored in these calculations). At $\psi \neq 0°$, the total reflex contour becomes significantly wider, and its center is shifted toward the short-wave range.

Reflex contour broadening can be explained by analyzing formula (2). Figure 7 shows an example of changes in the subgrating reflex wavelength for different values of θ_i and a specified angle of incidence of the probing beam $\psi = 10°$.

At $\psi = 0°$ (in the case of correlated conditions of hologram recording/reconstruction), the reflex wavelengths are identical for all values of θ_i and are equal to λ_0 (curve *1*), which should be expected from the physical viewpoint. According to formula (1), curve *2* describes the subgrating reflex wavelengths for the probing direction along the vector $\mathbf{G}_i$, i.e., it is assumed that $\psi = -\theta_i/2$. However, if $\psi \neq -\theta_i/2$, the probing beam is incident onto the subgratings at a certain angle with respect to the directions of their vectors, and the grating reflex wavelengths become smaller in accordance with formula (2). This reduction can be greater or smaller depending on the relationship of the signs of $\theta_i/2$ and ψ, which offers an explanation for the observed broadening of the contour of the total reflex spectrum (curve *3*) to the short-wave or long-wave range with respect to the point X corresponding to the center of the spectrum being considered.

DISCUSSION OF RESULTS

Thus, we found that the difference of the angle of incidence of the reference wave of white light from the direction of reference wave propagation during hologram recording in the case of volume reflection holograms of diffuse objects leads to broadening of the spectral response contour to both the short-wave and long-wave ranges. A theoretical explanation for this feature is proposed, and formulas for calculating the transmission spectra of the examined gratings are derived; the results predicted by these formulas are qualitatively consistent with experimental data.

Let us consider the formation of the resultant spectral response as a sum of reflexes of individual gratings in more detail.

Numbers *1*–*5* in Fig. 8a indicate the grating reflex spectra corresponding to object beams with the angles $\theta_i = 0$, ± 7.5, ± 15, ± 22.5, and $\pm 30°$ for $\psi = 0°$. According to formula (2), all reflexes have the same resonance wavelength. Simple summation of the reflection coefficients over the entire interval of i under consideration yields the values shown by curve *1* in Fig. 6.

A different pattern is observed for $\psi \neq 0°$. Figure 8b shows the data for gratings with object beams with $\theta_i = 0$, ± 1.5, and $\pm 40°$ for $\psi = 10°$. Obviously, the reflexes have different resonance wavelengths: curves *1* correspond to $\theta_i = 0$ and $\pm 1.5°$; curves *2* correspond to $\theta_i = \pm 40°$. As was noted above, the contribution of each individual reflex depends on the visibility V of the interference pattern for each subgrating. Gratings corresponding to small angles of scattering have a higher diffraction efficiency and make a greater

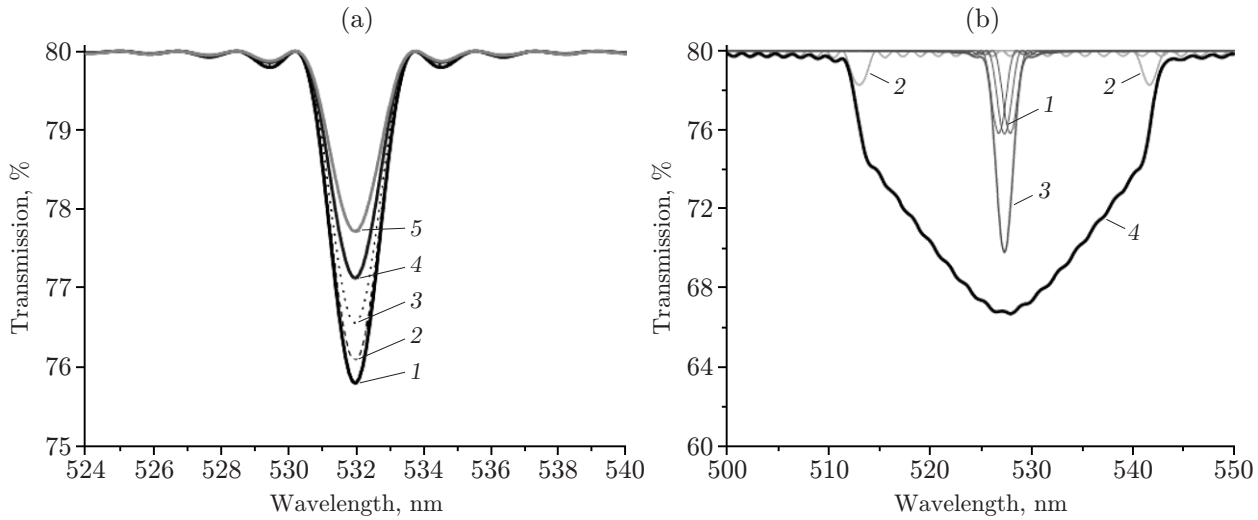

Fig. 8. Formation of the spectral response of the hologram as a sum of subgratings for different incidence angles of the probing beam: $\psi = 0^\circ$ (a) and $\psi = 10^\circ$ (b).

contribution. This is illustrated in the figure by curve *3*, which is a sum of reflexes at $\theta_i = 0$ and $\pm 1.5^\circ$, whereas the resultant reflex over the entire interval $\theta_i = +40, \ldots, -40^\circ$ is shown by curve *4*.

Thus, the observed spectral response of the volume reflection grating of the diffuse object under various probing conditions is always the sum of reflexes of subgratings with different spatial periods, reflected light directions, and diffraction efficiency levels.

Qualitative agreement of experimental and numerical data is obtained though there are also some differences. In the experiments, the central part of the reflex spectrum contours is sharpened, which may be related to incompleteness of the models of the angular distribution of scattered light and the spatial structure of the grating, in particular, this structure in real holograms may be inhomogeneous because of photopolymer shrinkage, there may be differences in Δn over the grating depth, etc. [14].

Based on the scheme [3], different reflection holograms were also fabricated, where the objects were a flat gypsum plate and a metallic object with a diffuse surface relief. The reflexes of these holograms demonstrated spectral properties close to those described above, but with some specific features associated with the presence of a large fraction of mirror reflection, which is manifested as sharpening of the reflex spectrum contour.

CONCLUSIONS

In the case of illumination of volume reflection holograms by white light, the conditions of their recording/reconstruction are often mismatched. The present experimental and theoretical investigations revealed broadening of the contour of the spectral response (reflex) of reflection holograms of diffuse objects to both short-wave and long-wave spectral ranges if the incidence angle of the reconstructing beam differs from of the reference beam direction in recording such holograms. This effect is essentially different from the known case [5] of the angular dependence of the reflex of an elementary volume reflection grating.

Based on the classical model of a periodic multilayered dielectric structure [13], formulas were derived for calculating the transmission spectra of reflection holograms, which were found to be qualitatively consistent with experimental data. It was demonstrated that their spectral response under various probing conditions is always a sum of reflexes of subgratings with different spatial periods, reflected light directions, and diffraction efficiency values.

The results of this work can be useful for design of art and security holograms, holographic displays, and for studying the properties of scattering/reflecting optical materials and functional structures on their basis.

The study was supported by the Russian Foundation for Basic Research and by the Government of the Novosibirsk Region within the framework of the research project No. 19-42-540005 entitled “Physical and experimental fundamentals of laser heterodyne tomography of internal properties of reflecting optical materials and structures.”

REFERENCES

1. H. Kogelnik, "Coupled Wave Theory for Thick Hologram Gratings," The Bell Syst. Techn. J. **48** (9), 2909–2947 (1969).
2. L. Solymar and D. J. Cooke, *Volume Holography and Volume Gratings* (Academic Press, London, 1981).
3. Yu. N. Denisyuk, "Recovery of Optical Properties of an Object in the Wave Field of Radiation Scattered by this Object," Optika i Spektroskopiya **XV** (4), 522–532 (1963).
4. *The Nobel Prize. Gabriel Lippmann.* https://www.nobelprize.org/prizes/physics/1908/lippmann/biographical/.
5. V. Kimberg, F. Gelmukhanov, H. Agren, et al., "Angular Properties of Band Structure of 1D Holographic Photonic Crystal," J. Opt. A: Pure Appl. Opt. **6** (10), 991–996 (2004).
6. J. A. Frantz, R. K. Kostuk, and D. A. Waldman, "Model of Noise-Grating Selectivity in Volume Holographic Recording Materials by use of Monte Carlo Simulations," JOSA **21** (3), 378–387 (2004).
7. R. A. Rupp and F. W. Drees, "Light-Induced Scattering in Photorefractive Crystals," Appl. Phys. B **39** (4), 223–229 (1986).
8. A. P. Yakimovich, "Estimation of the Influence of Secondary Scattering on the Diffraction Efficiency of Volume Holograms of Diffuse Objects," Kvant. Elektron. **10** (2), 332–336 (1983).
9. W. J. Gambogi, M. L. Armstrong, B. Hamzavy, et al., "Display Applications for Holographic Optical Elements," Proc. of SPIE **4296**, 312–318 (2001).
10. W. J. Gambogi, W. K. Smothers, K. W. Steijn, et al., "Color Holography using DuPont Holographic Recording Films," Proc. of SPIE **2405**, 62–73 (1995).
11. D. Jurbergs, F. Bruder, F. Deuber, et al., "New Recording Materials for the Holographic Industry," Proc. of SPIE **7233**, 72330K (2009).
12. S. Stevenson and W. Steijn Kirk, "A Method for Characterization of Film Thickness and Refractive Index in Volume Holographic Materials," Proc. of SPIE **2405**, 88–97 (1995).
13. M. Born and E. Wolf, *Principles of Optics*, Pergamon, Oxford (1975).
14. E. F. Pen, M. Yu. Rodionov, and V. V. Shelkovnikov, "Effect of Inhomogeneity of Volume Holograms in Photopolymer Materials on their Selective Properties," Opt. Zh. **73** (7), 60–65 (2006).